CONSTRAINING REGIONAL STRESS AND DEFORMATION AROUND BONAIRE AND THE BONAIRE BASIN: A SEISMIC REFLECTION STUDY

Collin Brandl, Bobby Reece

Department of Geology and Geophysics, Texas A&M University

GEOSCIENCES TEXAS A&M UNIVERSITY

10th Annual GGGSC Student Research Symposium

Poster No.

1. Introduction

The complex interactions between the South American and Caribbean tectonic plates are recorded in the basins surrounding the Netherlands Leeward Antilles, which is comprised of the islands of Aruba, Bonaire, and Curaçao (commonly referred to as the ABC Islands).

The island of Bonaire is located approximately 90 km north of Venezuela and sits in the center of the Bonaire Block. As the major plates move, this distinct crustal block deforms through faulting and folding (Fig. 1).

The Bonaire Block is bounded by the San-Sebastian and Oca-Ancon faults to the south, by the Los Roques Canyon to the east, and by the Curacao Ridge to the north.

Three general strike trends of faulting have been identified in the region: E-W striking normal faults, NW-SE striking normal faults, and WNW-ESE striking reverse faults *(Gorney et al. 2007)* (Fig. 2).

The present day stress state of the region is not well constrained. The goal of this study is to utilize seismic reflection data to place the Bonaire Block into the regional tectonic framework defined by previous studies.

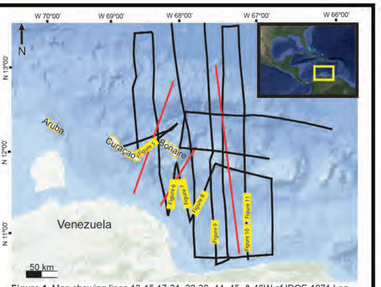

Figure 1. Map showing lines 13-15,17-21, 23-30, 44, 45, & 46W of IDOE 1971 Leg 4. Lines highlighted in red correspond to BOLIVAR lines 07,12, & 63 that were used to add age constraints. Image taken from Google Earth.

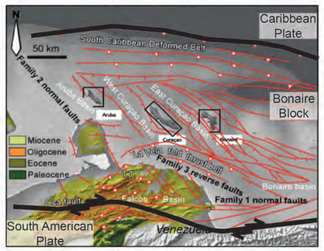

Figure 2. Tectonic map of the Leeward Antilles region with the Bonaire Block's north and south boundaries highlighted *(modified from Gorney et al. 2007)*.

2. Data/Methods

As part of the International Decade of Ocean Exploration, the United States Geological Survey (USGS) participated in an investigation of continental margins and basins in the Gulf of Mexico, the Caribbean Sea, and the western African continental shelf. Leg 4 of this cruise took place off of the northern coast of Venezuela in the continental borderland: in total 8,000 km of seismic data was collected (Fig. 1).

The data was acquired in approximately straight lines, numbered 1 - 49, and recorded on both film and paper. For our study we utilized lines 13-15, 17-21, 23-30, 44, 45, and the western portion of 46.

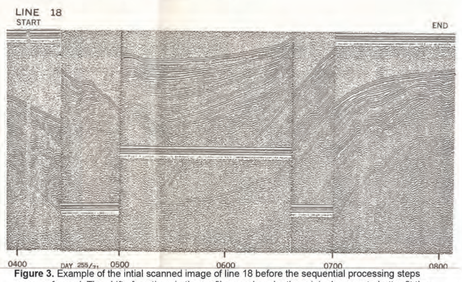

Figure 3. Example of the intial scanned image of line 18 before the sequential processing steps were performed. The shift of sections in the profile was done by the original survey to better fit the lines into the paper book. The numbered tick marks along the bottom provide hourly locations.

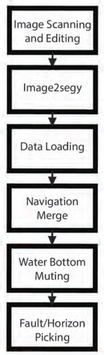

Figure 4. Processing flow used to convert scanned seismic images for this survey.

We used a special processing workflow to utilize the dataset (Fig. 4). This included specific Matlab software to convert scanned and edited images into SEGY files. We imported them into the Paradigm seismic processing suite and navigation was added to each line. We picked a waterbottom and then a mute was applied above it. Fault/horizon picking and interpretation was done using Paradigm Section.

3. Results

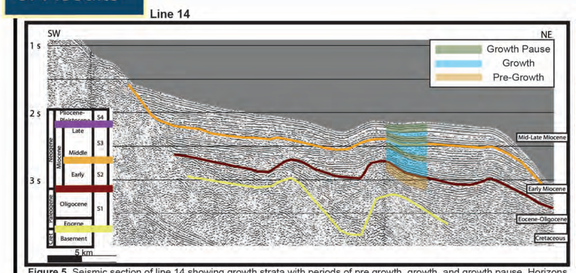

Figure 5. Seismic section of line 14 showing growth strata with periods of pre growth, growth, and growth pause. Horizons correspond to the top of seismic sequences modified from Gorney et al. 2007. Vertical exaggeration is 5x.

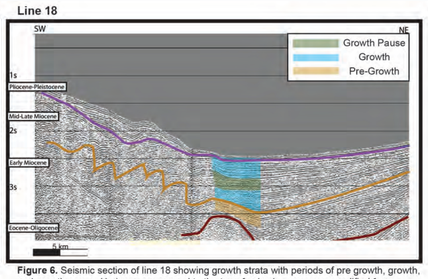

Figure 6. Seismic section of line 18 showing growth strata with periods of pre growth, growth, and growth pause. Horizons correspond to the top of seismic sequences modified from Gorney et al. 2007. Vertical exaggeration is 5x.

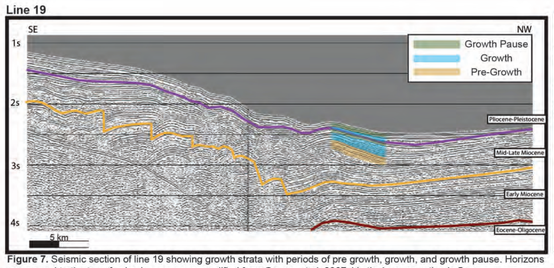

Figure 7. Seismic section of line 19 showing growth strata with periods of pre growth, growth, and growth pause. Horizons correspond to the top of seismic sequences modified from Gorney et al. 2007. Vertical exaggeration is 5x.

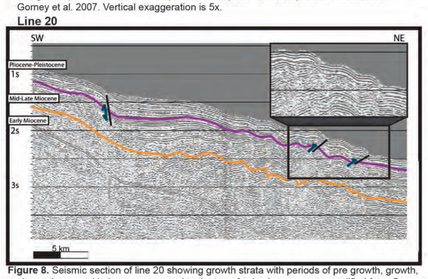

Figure 8. Seismic section of line 20 showing growth strata with periods of pre growth, growth, and growth pause. Horizons correspond to the top of seismic sequences modified from Gorney et al. 2007. Vertical exaggeration is 5x.

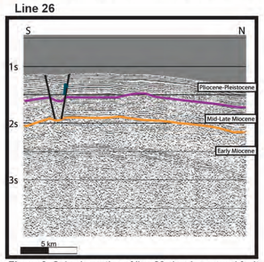

Figure 9. Seismic section of line 26 showing normal faults creating a collapse structure *(Silver et al. 1975)*. Horizons correspond to the top of seismic sequences modified from Gorney et al. 2007. Vertical exaggeration is 5x.

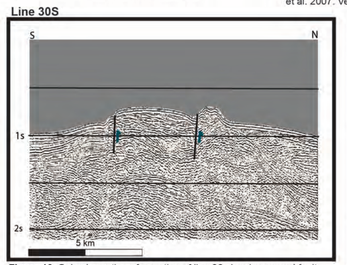

Figure 10. Seismic section of a portion of line 30 showing normal faults *(Silver et al. 1975)*. Vertical exaggeration is ~10x.

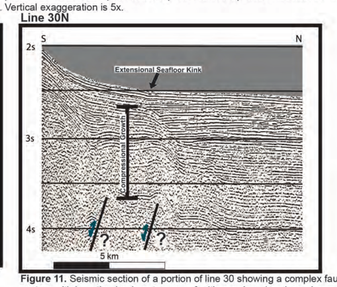

Figure 11. Seismic section of a portion of line 30 showing a complex fault system with hypothesized past reverse faulting and modern inversion. Vertical exaggeration is ~10x.

Observations

Line 14
Curved reflectors exhibit alternating periods of parallelism and divergence away from the axis of the fold. At the seafloor, the reflectors are parallel.

Line 18
Curved reflectors exhibit alternating periods of parallelism and divergence away from the axis of the fold. At the seafloor the reflectors are divergent.

Line 19
Curved reflectors exhibit alternating periods of parallelism and divergence away from the axis of the fold. At the seafloor the reflectors are parallel.

Line 20
Labeled lines show offset reflectors and resulting folds that break the seafloor. The left labeled line shows up-bending near the bottom and down-bending near the top.

Line 26
Collapse structure (Silver et al. 1975).
Structure shows downdrop in between the two labeled lines.

Line 30S
Normal faults (Silver et al. 1975).
Both offset the seafloor.

Line 30N
Folded and offset reflectors with a noticeable kink bend at the seafloor.

Based on our observations in the seismic sections, we interpret that:
The curved reflectors found on line 14 are an anticline with periods of growth and non-growth resulting from the movement of a subsurface fault. At the seafloor, the reflectors are parallel meaning the fault is not currently moving. (Fig. 5)

The curved reflectors present on line 18 and 19 are anticlines. The anticline on line 18 shows a growth pause at the seafloor while the anticline on line 19 shows growth at the seafloor. The growth at the seafloor is interpreted as a modern compressional stress regime. (Figs. 6,7)

The large set of offset layers that break the seafloor on line 20 are an inverted normal fault which implies a modern compressional stress regime. The other two sets of offset layers and folds are thrust faults that break the seafloor and also indicate a modern compressional stress regime (Fig. 8)

Silver et al. 1975 identified the collapse structure on line 26, formed from oppositely dipping normal faults, and the two normal faults on line 30 that offset the seafloor. These features are indicative of a modern extensional stress regime. (Figs. 9,10)

The kink bend in the seafloor also on line 30 could be the result of an inverted thrust fault or a recently moving normal fault. In either case, it indicates a modern extensional stress regime. (Fig. 11)

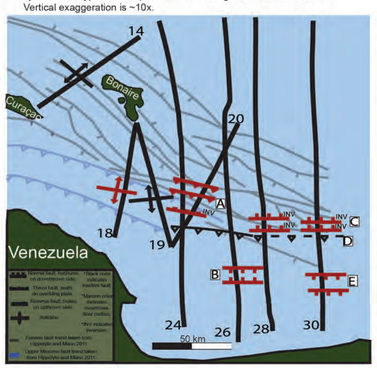

Figure 12. Map depicting locations of all interpreted faults and folds with growth strata.
A) Two labeled thrust faults breaking the seafloor and a single labeled reverse fault showing evidence of recent inversion.
B) Collapse structure breaking the seafloor (Silver et al. 1975).
C) Recently inverted reverse faults across lines 28 and 30 were identified by seafloor kink-bend and subsurface geometry. They share a similar location and appearance, but their connection is uncertain.
D) Observed subsurface folds and thrusts. Solid thrust line indicate confident inclusion into La-Vela Fold Thrust Belt. Dashed line indicates possible extent of La-Vela Fold Thrust Belt.
E) Normal faults breaking the seafloor (Silver et al. 1975).

4. Discussion

The anticline found on line 14 does not exhibit recent growth but could possibly represent an extension of the north anticline found with the high-resolution survey *(Bayer 2016) (Fig. 13)*.

The location of the anticlines present on lines 18 and 19 fit the previously established trend of compressional stress in the Upper Miocene for their location. However, the anticline portion on line 18 exhibits recent growth not observed on line 19. (Fig. 12).

The reactivated normal fault and thrust faults on line 20 that break the seafloor also indicate a present compressional stress regime. Additonally, they are present on line 24 and can be extrapolated across (Fig. 12).

The collapse structure on line 26 was caused by normal faults that break the seafloor, indicating a modern extensional stress regime.

The normal faults and seafloor kink bend found on line 30 are also indicative of a modern extensional stress regime.

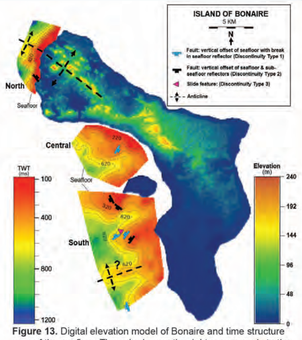

Figure 13. Digital elevation model of Bonaire and time structure map of the seafloor. The color bar on the right corresponds to the digital elevation model of Bonaire and indicates elevation in meters. The color bar on the left corresponds to the time structure maps of the seafloor off the west coast of Bonaire and indicates seismic two-way-travel time in milliseconds. The light gray dashed lines in the time structure maps of the seafloor represent 100 ms contour interval. *(From Bayer 2016).*

5. Conclusions/Future Work

We show that portions of our dataset fit previously established trends of regional deformation and stress. However, we also observe deformational features that do not fit the previously established trends:

Figure 14. Portion of high-resolution seismic line a nearshore Bonaire survey. The hard-bottom seafloor prevents energy penetration and results in minimal subsurface imaging. *(From Bayer 2016).*

• We interpret the modern stress trend across the survey region to be non-uniform with compression to the west and extension to the east.

• **Our findings could support previous conclusions of regional transpression causing stress orientations resembling simple shear (Gorney et al. 2007), or clockwise block rotation about an onshore pole (Silver et al. 1975).** However, the true trends of faulting are needed for further comparison. Our findings do not fit results indicating modern, uniform regional extension (Hippolyte and Mann 2011) but local findings around Bonaire (Bayer 2016) could fit our proposed framework.

• **We propose a modern tectonic mechanism that combines simple shear and rotation; the Caribbean plate drives the Bonaire Block eastward while right lateral slip along the Oca-Ancon fault system resists the motion.** Pure simple shear would not completely explain lateral variation in faulting and pure clockwise rotation is not occuring because the Oca-Ancon fault system is right lateral (Fig. 2).

Future work will include:
• Work to further correlate study results with the high resolution survey. Difficulty arises due to the difference in survey scale (regional versus local) and seafloor penetration. Large features are not distinct in the high resolution dataset due to the short length of the survey lines. The hard bottom seafloor prevented the high resolution survey from imaging less than a few meters into the crust.

•Examine other possible tectonic mechanisms that would result in the non-uniform stress regime and refine our proposed mechanism.

References/Acknowledgements

Special thanks to the Texas A&M University College of Geosciences for the financial support of undergraduate research and to Paradigm for the donation of seismic processing and interpretation software.

•Bayer, J., 2016, Structural Analysis of Bonaire, Netherlands Leeward Antilles-A Seismic Investigation [Masters Thesis]: Texas A&M University, p. 107

• Gorney, D., Escalona, A., Mann, P., Magnani, M. B., and Group, B. S., 2007, Chronology of Cenozoic tectonic events in western Venezuela and the Leeward Antilles based on integration of offshore seismic reflection data and on-land geology: AAPG Bulletin, v. 91, no. 5, p. 653-684.

• Hippolyte, J.-C., and Mann, P., 2011, Neogene–Quaternary tectonic evolution of the Leeward Antilles islands (Aruba, Bonaire, Curaçao) from fault kinematic analysis: Marine and Petroleum Geology, v. 28, no. 1, p. 259-277.

• Silver, E. A., Case, J. E., and MacGillavry, H. J., 1975, Geophysical study of the Venezuelan borderland: Geological Society of America Bulletin, v. 86, no. 2, p. 213-226.